

國立交通大學

電子工程學系電子研究所

碩士論文

應用寫入輔助電路之低功耗雙埠
靜態隨機記憶體之測試方法

Test Methodology for

Low-Power Dual-Port SRAM Utilizing Write-Assist Cells
Against Simultaneous Access Disturbance

研究生：黃召穎

指導教授：趙家佐

中華民國一〇二年九月

應用寫入輔助電路之低功耗雙埠

靜態隨機記憶體之測試方法

Test Methodology for
Low-Power Dual-Port SRAM Utilizing Write-Assist Cells
Against Simultaneous Access Disturbance

研究生：黃召穎 Student : Chao-Ying Huang

指導教授：趙家佐 Advisor : Mango Chia-Tso Chao

國立交通大學

電機學院 電子工程學系 電子研究所

碩士論文 1996

A Thesis

Submitted to Department of Electronics Engineering & Institute of Electronics
College of Electrical and Computer Engineering

National Chiao Tung University

In partial Fulfillment of the Requirements

for the Degree of

Master

in

Electronics Engineering

August 2013

Hsinchu, Taiwan, Republic of China

中華民國一〇二年九月

應用寫入輔助電路之低功耗雙埠

靜態隨機記憶體之測試方法

研究生：黃召穎

指導教授：趙家佐

國立交通大學

電機學院

電子工程學系

電子研究所

摘要

隨著多核心運算及平行化處理需求漸增，雙埠靜態隨機記憶體在提高效能上的優勢逐漸顯著。另一方面由於記憶體應用層面逐漸由傳統桌上型電腦轉移到行動裝置等相關產品，因此以低功耗操作和高速存取為目標的記憶體設計更是蓬勃發展。然而在先進製程中嚴重製程變異使製造過程中的穩定性相對降低，以及在追求低功耗操作及高速的存取的情況下，雙埠靜態隨機記憶體的讀取及寫入更加顯得不穩定。上述的不穩定性導致雙埠隨機靜態記憶體在低功耗操作上更顯困難。為了保持可接受的讀取及寫入能力配合降低操作電壓達到低功耗的目的，許多讀取及寫入的輔助電路在各個製程下逐漸被提出使用。本論文著重於討論雙埠靜態隨機記憶體配合寫入輔助電路幫助下之開路缺陷的錯誤行為模式並提出相對應的測試方法。此輔助電路應用於解決雙埠靜態隨機記憶體在先進製程下受到嚴重製程變異使寫入能力衰減嚴重的情況。

Test Methodology for
Low-Power Dual-Port SRAM Utilizing Write-Assist Cells
Against Simultaneous Access Disturbance

Student: Chao-Ying Huang Advisor: Mango Chia-Tso Chao

Department of Electronics Engineering and Institute of
Electronics National Chiao-Tung University

Abstract

With the increasing demand of parallel applications and multi-core operations, the advantages of Dual-Port SRAMs have become more important. Also, applications of SRAMs have moved from the traditional desktop to the mobile device; therefore, the designs which are aimed at low-power operations and high-speed accesses are currently prospering. Besides as process variation in the advanced technology becomes more severe, the stability of SRAMs in data retention mode and read/write operation has become more fragile. The low stability property may cause Dual-Port SRAMs unable to operate at low voltage. In order to maintain an acceptable read/write margin with low power issue, some read/write assist circuitries have been proposed recently. As a result, the thesis emphasizes on the fault behaviors of open defects for Dual-Port SRAMs with specific write-assist circuitry and its corresponding test methodologies for those hard-to-detect faults.

Acknowledgements

First and foremost, I would like to express my greatest appreciation to my advisor, Professor Chia-Tso Chao (Mango, 趙家佐). He is not only a teacher but also a life mentor to me. He is always there when I am at the crossroad of my life, and guides me with clear and useful advices. He expects me to be a man not only with professional skills but with a positive attitude toward challenges. I would never become who I am today if it were not for him. It is my honor to meet a friend-like teacher as Professor Chao. Second, I'd like to thank my upperclassmen, Jhen-An Lai. He gives me opportunities to work as an intern in TSMC and helps me get over the difficulties in this work. Everything I learned from him is a great treasure in my life. I will always keep that in mind and be thankful forever. Third, I'd like to thank my lab-mates: Hao-Yu Yang, Cheng-Wei Lin, Sz-Pang Mu, Yu-An Chen and all the others. Without their assistance, I would not be able to deal with the academic works and the arduous research tasks smoothly during the past two years. Last, I appreciate my dear parents and my girlfriend, Michelle, for their support and encouragement all these years. It is your immense love that keeps me fighting hard. I hope that this work makes you proud.

Chao-Ying Huang

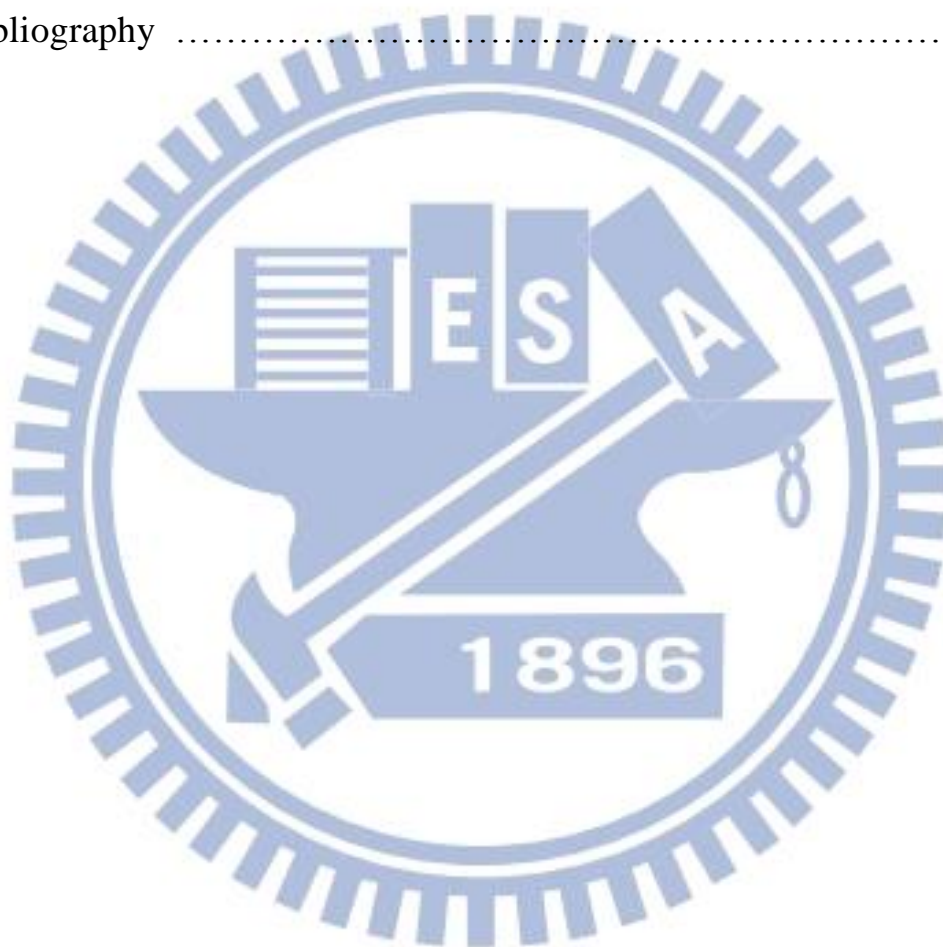
National Chiao-Tung University

2013, September

Contents

中文摘要	I
English Abstract	II
Acknowledge	III
List of Tables	VI
List of Figures	VII
1 Introduction	1
2 Write-Assist Dual-Port SRAM and the Fault Behaviors	3
2.1 Background of Write-Disturb Issue	5
2.2 Write-Assist Circuitry and Its Operations	8
2.2.1. Background of Write-Assist Circuitry	8
2.2.2. Write-Assist Circuitry Operations	9
2.2.3. Write-Assist Circuitry Control	10
2.3 Fault Behaviors of DP-SRAMs and Write-Assist Circuitry	11
2.3.1 Background of Stability Faults	11
2.3.2 Macro Implementation	12
2.3.3 Fault Behavior for Dual-Port SRAM Cells	13
2.3.4 Fault Behaviors for Write-Assist Circuitry	20
3 Testing of Write-Assist Dual-Port SRAM and the Proposed Methods	22
3.1 Testing of the Open Defects in Dual-Port SRAM Core Cell	23
3.1.1 Previous Method – Severe Write Method	23
3.1.2 Proposed Method – Half-VDD Attacking Method	25
3.1.3 Experiment Results and Comparison	26
3.2 Testing of the Open Defects in Write-Assist Circuitry	29
3.2.1 Proposed Method – Low-Voltage Write-Assist Method	29

3.2.2	Proposed Method – Severe Read Method	30
3.2.3	Experiment Results and Comparison	31
3.3	Design-for-Test for the Proposed Methods	33
3.3.1	DFT for Half-VDD Attacking Method	33
3.3.2	DFT for Low-V Write-Assist Enable Method	35
4	Conclusion	37
5	Bibliography	39



List of Tables

Table 2-I	Cross Combinations of Different Discussed Conditions	13
Table 2-II	Fault Behaviors of Open Defects for Confiruation-1 and Sub-Category1&2	16
Table 2-III	Fault Behaviors of Open Defects for Confiruation-2 and Sub-Category1&2	16
Table 2-IV	Fault Behaviors of Open Defects for Confiruation-3 and Sub-Category1&2	17
Table 2-V	Fault Behaviors of Open Defects for Confiruation-3 and Sub-Category3	19
Table 2-VI	Fault Behaviors of Open Defects for the Write-Assist Circuitry (WA8T)	21
Table 3-I	Effectiveness of Different Test Methods for the S/D Open Defect of Sub-Category1&2	28
Table 3-II	Effectiveness of Different Test Methods for the S/D Open Defect of Sub-Category3 for Configuration3	29
Table 3-III	Experiment Result for the Gate Terminal Open Defect of the WA8T	32
Table 3-IV	Experiment Result for the S/D Terminal Open Defect of the WA8T	33
Table 3-V	Half-VDD Attacking Operating Flow	34
Table 3-VI	Comparisons of Voltage State for Half-VDD Attacking	35
Table 3-VII	Operations of Low-V Write-Assist	36

List of Figures

Fig. 2-1 Illustration of DP-SRAM and VDD_{min} Penalty [2-1]	5
Fig. 2-2 Waveform of Write Disturbance [2-1]	6
Fig. 2-3 Waveform of Write Disturbance for Different Skews [2-4]	7
Fig. 2-4 Structure and Schematic of DP-SRAM and the WA8T [2-1]	8
Fig. 2-5 Simulated Waveform of the W-R Operation [2-1]	10
Fig. 2-6 Illustration Waveform of the WAEN Signal	10
Fig. 2-7 Schematic of Dual-Port SRAM Cell	14
Fig. 2-8 Schematic of the Write-Assist Circuitry (WA8T)	20
Fig. 3-1 Illustration of Severe Write Method[2-11]	24
Fig. 3-2 Illustration of Half-VDD Attacking Method	26
Fig. 3-3 Illustration of Severe Read Method	31
Fig. 3-4 Illustration of the DFT for Half-VDD Attacking	34
Fig. 3-5 Illustration of the DFT for Low-V WAEN	36

Chapter 1

Introduction

Parallelism has been the one of the most important principles to increase a system's throughput in the past. With the continually decreasing price and increasing performance of silicon chips for each new process generation, incorporating multiple processors into a system has become a more feasible, effective, and economic solution to further explore the computation parallelism of a system as well as its throughput. The performance of a multiple-core system can be significantly affected by the following two major factors: (1) the bandwidth of its memory and (2) the bandwidth of its communication between different cores. To improve the memory bandwidth and the communication bandwidth, significant research efforts have been put into the area of multi-port SRAM designs and network-on-chip (NOC) designs in the past, respectively. Designing a multi-port SRAM to provide multiple paralleled accesses to the same data array is an effective solution to increase the memory bandwidth. Dual-port SRAMs are the most commonly used multi-port SRAMs nowadays, providing two individual ports which can perform either a read or a write operation independently.

On the other hand, due to the increasing demand of low-power system, a great amount of research effort has been spent in the past to develop the effective and economic designs so as to operate with low supply voltage.

However, Dual-Port SRAMs suffer disturb issues in advanced technology nodes owing to its dual-port access nature. These disturb issues may degrade the minimum operating voltage of Dual-Port SRAMs. Therefore, many read-/write-assist circuits have been proposed to circumvent these disturb issues. Accordingly test methods regarding those newly developed Dual-Port SRAM designs and assist circuitries have not been fully discussed yet.

In the chapter 2, we first discuss the reasons that cause the write disturbance for Dual-Port SRAMs in detail and we talk about the write-assist circuitry used in this work later, including the basic operation of it and its timing controls. We then move to the discussion of defect injection part. We show the experiment results of the measured resistance for each open defect from the table 2-I to the table2-V. By observing the results, we aim our targets at the larger resistance detects and we propose our own test methodologies in the next chapter.

In the chapter 3, we introduce the previous methods proposed by others that relate to our targets and our proposed method as well. The followings are our proposed methods. Half-VDD attacking method is used for the defects in Dual-Port SRAM Cell and low-voltage write-assist method and severe read method are used for the defects in the write-assist circuitry independently. Later, we show the comparison table of the measured results to prove that our methods are in good use. In the end, we discuss Design-For-Test of the proposed methods to prove that our methods are applicable. In the chapter 4, we make a brief conclusion about our work. In chapter 5, we talk about the future work of this research.

Chapter 2

Write-Assist Dual-Port SRAM and the Fault Behaviors

In deep sub-micrometer technology, system-on-chip (SoC) products require a high-speed and low-power embedded memory to support increased storage capability. Therefore, dual-port static random access memory (DP-SRAM) has been widely used for SoC products such as graphic and media processing chips. In order to obtain low-power target, low supply voltage method has been widely used for these advanced applications. However, utilizing low supply voltage to achieve power reduction for DP-SRAMs is susceptible to variations in the threshold voltage (V_{TH}). These variations might result from random doping fluctuations and lithography processes, which cause a subsequent reduction in the VDD_{min} performance of SRAMs. For DP-SRAMs, the VDD_{min} is even more fragile when discussing whether one- or two- port operation is enabled, especially when it is operated at the dual-port access. In this chapter we will discuss the background of DP-SRAM operations and the write-disturb issue. We implement the DP-SRAM macro and observe the repairing mechanism of the write-assist circuitry at first. Then we analyze the effects causing by the open defect on the gate or the source/drain terminal later.

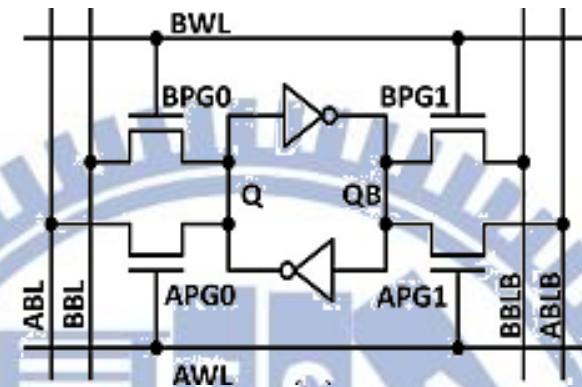
Figure 2-1(a) shows a schematic of the DP-SRAM. There are two different word-lines (AWL and BWL) controlling different-port operations. For each

operation, they determine the corresponding electrical connection between storage nodes (Q and QB) and bit-line pairs (ABL/ABLB and BBL/BBLB). A DP-SRAM macro has two independent timing control circuits and address decoders respectively and these two independent ports can be operated simultaneously. Hence, DP-SRAMs suffer “disturb issue” when both ports are accessed at the same row. The disturb issue can be classified into read-disturb issue and write-disturb issue. The extent of each disturb issue is related to the timing skew of different clock phase. Figure 2-1(b) shows that the worst V_{\min} condition occurs when some clock difference exists. In this work, we focus on write disturb issue which has more severe VDD_{\min} degradation problem in short word-line pulse for high speed applications.

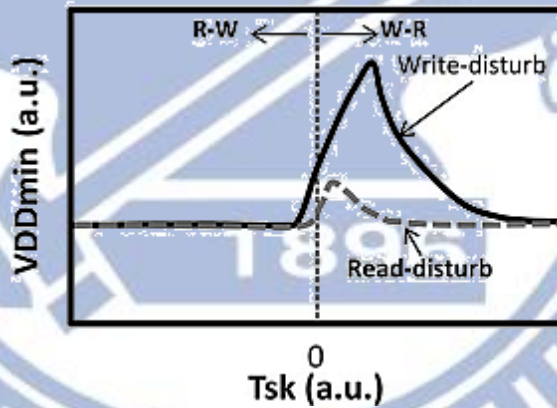
From Figure 2-1 (b), the positive timing skews (T_{sk}) happen when activating the write word-line before the read word-line (W-R operation) and it causes a great degradation in VDD_{\min} ; in contrast, the negative timing skews (T_{sk}) happen when activating the read word-line before write word-line (R-W operation) and it causes no clear degradation in VDD_{\min} . For this reason, W-R operation in the same row is the major concern for the write-disturb issue.

To overcome the disturb issue and successfully operate DP-SRAMs at lower VDD_{\min} , some new assist circuitry designs for read or write operations have been proposed. Tackling the read-disturb issue, which causes degradation in read static noise margin on 65nm technology node, [2-2] proposed a bit-line shifter circuit and row address comparator to prevent common-row-access operation. For the write-disturb issue, [2-1], [2-3] and [2-5] proposed the write-assist circuit to achieve a lower VDD_{\min} with low area overhead and power consumption on either 45nm or 28nm technology node. [2-4] even analyzed the read-/write- disturb issue under different timing skews and proposed a screening

circuitry to allow us to generate the read-/write- disturb condition without conventional costly operations. We select [2-1] as the write-assist circuitry in the following work, because it is not only the newest write-assist circuitry but with minimum area overhead as well.



(a) Cell Structure of the DP-SRAM cell



(b) $V_{DD_{min}}$ Penalty versus AWL-BWL Timing Skew

Fig. 2-1 Illustration of DP-SRAM and $V_{DD_{min}}$ Penalty [2-1]

2.1 Background of Write-Disturb Issue

When V_{TH} variations happen, the unbalanced driving ability of cross-coupled inverter and pass-gate transistors of DP-SRAM cell may make the cell prefer to

specific read or write operation. This situation is even more severe in advanced process, such as 40nm or 28nm technology. Moreover, simultaneous row access behaviors degrade the read/write margin seriously and the synchronization of the timing of different word-lines is also important in low supply voltage condition.

Figure 2-2 shows a simulated waveform of DP-SRAM cell storing logic-1 under A-port write and B-port read operation (W-R). There exist some timing skews between two different clock phases: A-port in the write mode with earlier access and B-port in the read mode with later access. The write operation can be divided into four stages, T1 to T4. In the stage T1, only the write port is turned on (AWL on) and the pull-down speed of the voltage at the node Q depends on the discharge current from A-port pass gate. In the stage T2, both the write and the read operation are on (AWL on & BWL on). BBL injects charges into the node Q, which considerably reduces the pull-down speed of it. In the stage T3, the write operation is off (AWL off) and the node Q discharging operation is halted while B-port continues charging the node Q. In the stage T4, as long as the node Q does not reach the write-trip-point of the cross-coupled inverter at the end of stage T3, the node Q will be pulled back to VDD by the cross-coupled inverter whereupon write failure occurs.

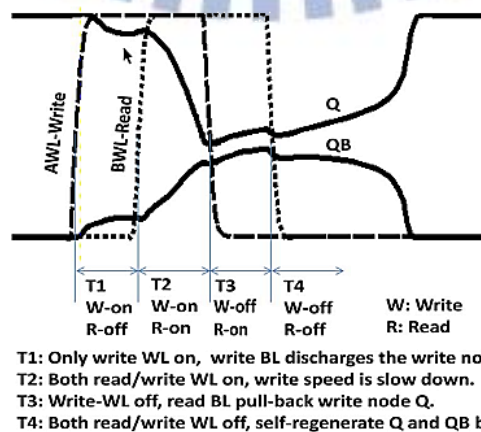


Fig. 2-2 Waveform of Write Disturbance [2-1]

The timing skews between different word-lines are also important for the write-disturb issue. Figure 2-3 shows the comparison waveform of the timing skews for the simultaneous row access of DP-SRAM cell. The notation MT and MB stand for two complementary storage nodes. A-port is for write-logic-0 operation and B-port is for read-operation (or half-selected read) in this example. Figure 2-3(a) corresponds to negative skews, figure 2-3(b) corresponds to zero skew, figure 2-3(c) corresponds to positive skews and figure 2-3(d) corresponds to amount of positive skews between word-lines. Regarding figure 2-3(a) and figure 2-3(b), although the MT suffers the write-disturb issue, the write operation is success owing to its inherent cell ability to flip the internal data. However, in figure 2-3(c), the MT is kept on ramping up by BLB after WLA is off, which eventually results in the write failure. With regard to figure 2-3(d), where the amount of positive skew is larger than figure 2-3(c), MT flips immediately because the write-disturb issue starts appearing after the write operation is finished. To sum up, figure 2-3(c) produces the worst-case scenario, which needs effective write-assist circuitry to repair during the write operation.

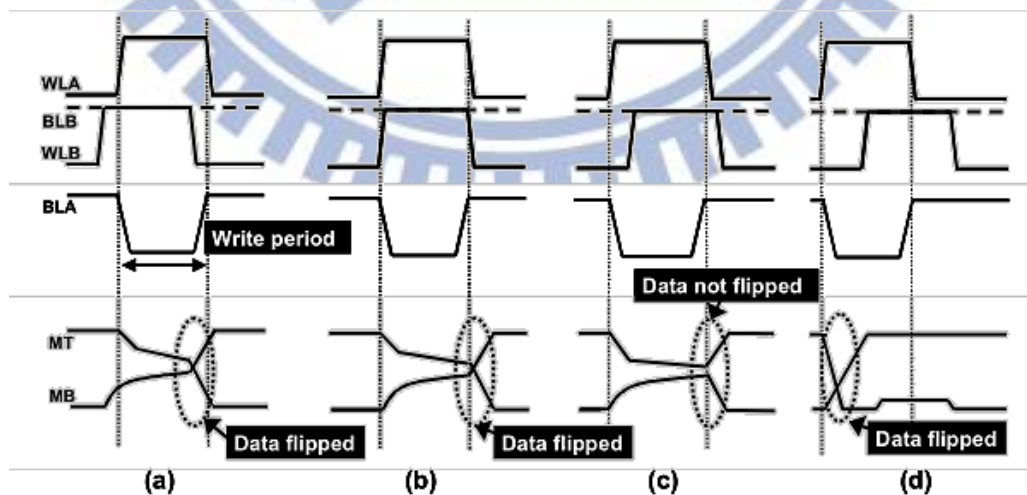


Fig. 2-3 Waveform of Write Disturbance for Different Skews (a) negative skew (b) zero skew (c) positive skew (d) amount of positive skew [2-4]

2.2 Write-Assist Circuitry and Its Operation

2.2.1 Background of Write-Assist Circuitry

Figure 2-4 shows the structure of DP-SRAM using the proposed write-assist circuitry from [2-1], which is noted as the WA8T cell. It achieves a lower VDD_{min} by suppressing the write disturbance with small area overhead and low power consumption. The circuitry is formed by two inverters (INV1 and INV2) and two stacked-NMOS bit-line pull down drivers (N1-N2 and N3-N4 pairs). The write-assist enable signal (WAEN) controls the N1 and N3 transistor to determine when the WA8T cell should be turned on.

According to [2-1] states, SRAMs usually require edge dummy cells to ensure a uniform layout in the middle and edges of the cell array. The proposed WA8T cell uses the poly and diffusion layout pattern of regular DP-SRAM cells, which facilitates the proximity effect of the DP-SRAM edge dummy cells. Therefore, with cells placed in the same locations along the top/bottom edge of dummy cells, the proposed the WA8T cell has almost no area penalty.

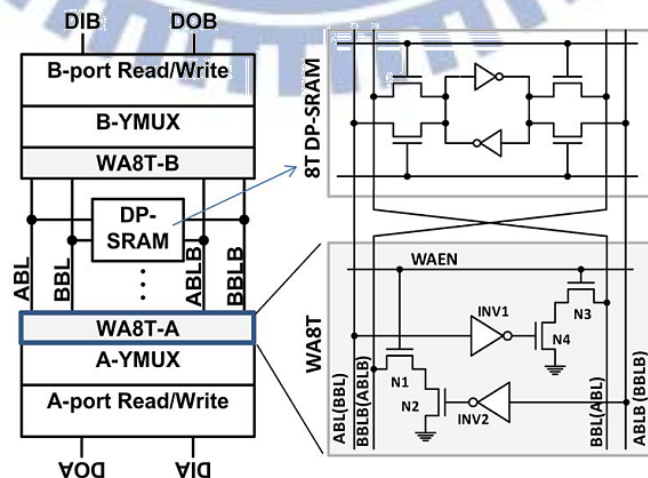


Fig. 2-4 Structure and Schematic of DP-SRAM and the WA8T [2-1]

2.2.2 Write-Assist Circuitry Operations

Figure 2-5 shows an example that how the WA8T cell helps to suppress the write disturbance through a W–R operation in DP-SRAM cell. In the operation, two word-lines are accessed at the same row with independent operations: A-port is for write-logic-0 and B-port is for read operation (or half-selected read). ABL is pulled down to ground and ABLB is maintained at VDD by the write driver of A-port, while both BBL and BBLB are at VDD at the beginning of BWL. It can be seen that DP-SRAMs without the WA8T cell may suffers the write-disturb issue causing write-logic-0 operation failed at the end of AWL. Eventually, cross-couple inverters pull back the node Q to VDD resulting in the write failure.

On the other hand, DP-SRAMs with the WA8T cell would pass the write operation under the write-disturb issue. The INV1 senses the logic-0 at ABL and outputs a logic-1 at the gate of N4. The INV1 senses the logic-1 at ABLB and outputs a logic-0 at the gate of N2. When the WAEN signal for A-port WA8T cell is active, the N3–N4 stacked-NMOS driver begins discharging BBL and the N1–N2 driver is in a state of high impedance (N2 is off). The B-port WA8T cell remains inactive by keeping its WAEN signal off. The reduced voltage at BBL helps to suppress the write disturbance caused by B-port being pulled high in the conventional approach. Moreover, the WA8T cell not only suppresses the write-disturb issue but also improves the write margin owing to the additional write path of the other port (B-port in this example).

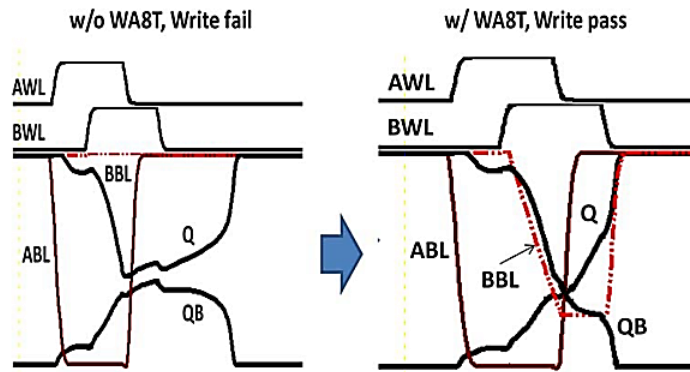


Fig. 2-5 Simulated Waveform of the W-R Operation [2-1]

2.2.3 Write-Assist Circuitry Control

The write-assist enable signal (WAEN) of the WA8T cell is implemented in the A-/B- port timing control circuits independently. Figure 2-6 illustrates the timing of the WAEN signal. The WAEN signal remains at logic-0 level (inactive) under all conditions except the W–R operation at the same row. Moreover, if AWL and BWL are in the non-overlapping region, the WAEN signal also remains at logic-0 level even for the W–R operation. Note that the WA8T cell should be disabled (WAEN = logic-0) for the R–W operation. If the WA8T cell is activated during the R–W operation (B-port read and A-port write), the WA8T cell will transfer the B-port read data to the ABL and the ABLB, resulting in data conflict.

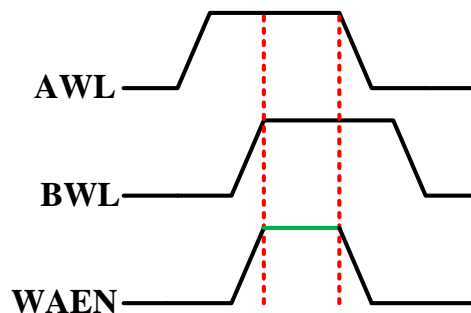


Fig. 2-6 Illustration Waveform of the WAEN Signal

2.3 Fault Behaviors of DP-SRAMs and Write-Assist Circuitry

2.3.1 Background of Stability Faults

A stability fault defined in [2-6]-[2-7] refers to a small open defect on the source/drain terminal of four cross-coupled transistors, which may not fail a read or a write operation under a typical operating condition but may fail under some corner conditions (such as significant IR drop, noise, or soft error). As a result, a stability fault may decrease the reliability of SRAM but may not be easily detected by a conventional march sequence. Therefore, testing stability faults has become one of the most challenging tasks in current SRAM testing. Several test methods were proposed to detect the stability faults with as small resistance as possible, [2-6]-[2-9].

For traditional 6T SRAMs, the past research effort mainly focused on the stability faults located on the source/drain terminal of pull-up PMOS transistors and ignored the stability faults locating on pull-down NMOS transistors, which can be detected relatively easily by the read operation because the bit-lines in general SRAMs operations are pre-charged to VDD before a read operation. If the NMOS transistors cannot successfully pull down the bit-line due to the open defects, the pre-charged value (floating logic-1) will be read out, which is opposite to the expected value. On the other hand, if the PMOS transistors cannot successfully pull up the bit-line due to an open defect, the pre-charged value (floating logic-1) just happens to be the expected value making the open defect not detect.

For DP-SRAMs, [2-10] states that it can be divided into single-port faults (1PFs) and two-port faults (2PFs). The 1PFs can be detected using the

conventional single port memory tests. However, through our experiment, we found that open defects for stability faults located on the source/drain terminal of pull-up PMOS transistors are still hard to detect. We focus on 1PFs in the following part and the 2PFs requiring special test methods are not involved in this work.

2.3.2 Macro Implementation

We implement a DP-SRAM macro on 28nm technology node with 128 cells per column and per row. The sizing of the DP-SRAM cell is based on [2-2] so as to make the cell with weak read-ability and weak write-ability. The capacitance on each bit-line is 20 fF, which is suggested by our cooperated industries. We use 2-stage row decoder and mux8 tree-based column decoder. The sense amplifier we use is a latch type sense amplifier. We operate the macro at 0.75V which is lower than its standard supply voltage, 1.05V, to realize low power application. As stated before, the write-disturb issue occurs when there exists variations in threshold voltage (V_{TH}) and some positive word-line skews. Therefore, we carry out three different cell-sizing and run Monte-Carlo simulations to verify that for each cell-sizing the single-port access can work successfully and the simultaneous dual-port access would fail. In order to observe the open defects in the WA8T cell, we select seven V_{TH} variation conditions on cell-sizing-3 and use the WA8T cell to repair the write-disturb issue as stated in [2-1]. For both the DP-SRAM macro and the WA8T cell, we proceed to perform the defect injection exhaustively and use different test methods to detect the minimum resistance.

The experiments can be divided into two main categories:

- Category1: Open Defects occur in DP-SRAM cell.
- Category2: Open Defects occur in the WA8T cell.

The category1 can be divided into three sub-categories. Each sub-category represents one cross-combination of with/without V_{TH} variation and with/without the WA8T cell in table 2-I. We do not discuss the situation when DP-SRAMs with V_{TH} variations and without write-assist circuitry simultaneously, because DP-SRAMs can not operate correctly even for defect free condition.

TABLE 2-I
Cross Combinations of Different Discussed Conditions

	w/ V_{TH} Variations	w/o V_{TH} Variations
w/ Write-Assist Circuitry	Sub-category3	Sub-category2
w/o Write-Assist Circuitry	Not in discussion	Sub-category1

2.3.3 Fault Behaviors for Dual-Port SRAM Cells

In the following experiments, we inject an open defect with different resistance value one at a time on each terminal (gate or source/drain) of each transistor, as shown Figure 2-7. By sweeping all single-port read/write operations and all dual-port write-read operations, we report the minimum resistance for each open defect, which can cause a fault behavior for DP-SRAM design, shown in table 2-II to Table 2-IV. In order to observe whether the open defect for DP-SRAM cells will be affected by the V_{TH} variation and the WA8T cell or not, we define three sub-categories as stated in section 2.3.2. We first

discuss experiment results of sub-category1 and sub-category2 together to compare the influence of with/without write-assist circuitry and then we discuss the sub-category3 to compare the influence of different V_{TH} variations in cell-sizing-3.

From Table 2-II to Table 2-IV list the minimum detectable resistance of each open defect (Column 5) and the fault behavior (Column 4) for three configurations of the sub-category1 and the sub-category2. Note that we add one open defect, RQ, between the left storage node Q and right storage node Q and another open defect, RQB, between the left storage node QB and right storage node QB. These two open defects may cause the cross-couple inverter unable to link together resulting in the read/write failure. In addition, once the defect can generate a read failure or a write failure, the open defect can be easily detected by a conventional SRAM march sequence. Therefore, we only need to consider the open defects with fault-resistance less than the minimum detectable resistance.

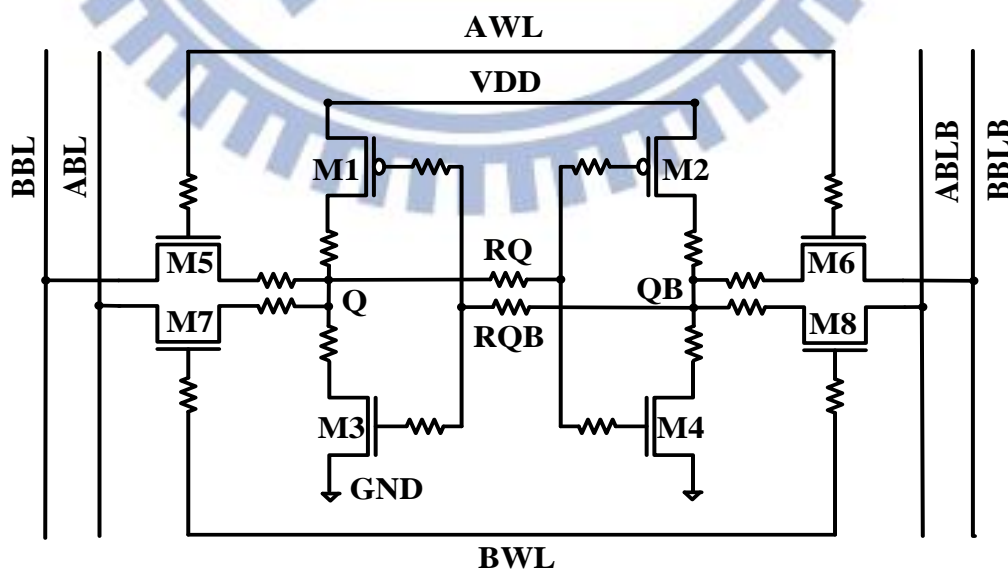


Fig. 2-7 Schematic of Dual-Port SRAM Cell

We demonstrate that the open defects located on the DP-SRAM cell (M1 to M8) all fail on the single-port or the dual-port write operation from Table 2-II to Table 2-IV. These defects are classified as stability faults in Section 2.3.1. Apparently, the open defects located on the gate terminal are detected by a larger resistance. We infer that it is mainly related to its inherent high impedance nature of the device structure. On the contrary, most open defects locate on the source/drain terminal are easy to detect except those on the source/drain terminal of the pull-up transistors. Similar to traditional 6T SRAMs, stability faults on PMOS transistors (M1 and M2) are hard to detect and stability faults on NMOS transistors can be detected with two-order less for category-1 and category-2. This result states that detecting stability faults on PMOS transistors is more critical than on NMOS transistors for DP-SRAM cell without V_{TH} variations. From Table 2-II to Table 2-IV, we note that category-1 and category-2 have similar minimum detectable resistance for each open defect. We can conclude that the write-assist circuitry has no great influence on testing DP-SRAM cells with little or no V_{TH} variations.

TABLE 2-II
Fault Behaviors of Open Defects for Cell-Sizing-1 of Sub-Category1&2

Property	Transistor Name	Transistor Terminal	Faulty Behavior	Min. Detectable Resistance Of Sub-Category1	Min. Detectable Resistance Of Sub-Category2
A-port pass transistor	M5	G	(SP) A-Port W0 Failed	6 MΩ	7 MΩ
		S/D	(SP) A-Port W1 Failed	50 KΩ	100 KΩ
	M6	G	(SP) A-Port W1 Failed	6 MΩ	7 MΩ
		S/D	(SP) A-Port W0 Failed	50 KΩ	100 KΩ
B-port pass transistor	M7	G	(SP) B-port W0 Failed	3 MΩ	3 MΩ
		S/D	(SP) B-port W1 Failed	50 KΩ	60 KΩ
	M8	G	(SP) B-port W1 Failed	3 MΩ	3 MΩ
		S/D	(SP) B-port W0 Failed	50 KΩ	60 KΩ
Pull-Up transistor	M1	G	(SP) A-Port W0 Failed	4 MΩ	6 MΩ
		S/D	(SP) A-/B-port W1 Failed	20 MΩ	30 MΩ
	M2	G	(SP) A-Port W1 Failed	4 MΩ	6 MΩ
		S/D	(SP) A-/B-port W0 Failed	20 MΩ	30 MΩ
Pull-Down transistor	M3	G	(SP) A-/B-port W1 Failed	2 MΩ	3 MΩ
		S/D	(DP) A-port W0 Failed	300 KΩ	500 KΩ
	M4	G	(SP) A-/B-port W0 Failed	2 MΩ	3 MΩ
		S/D	(DP) A-port W1 Failed	300 KΩ	500 KΩ
Connection	RQ	-	(SP) A-/B-port W0/W1 Failed	700 KΩ	700 KΩ
Connection	RQB	-	(SP) A-/B-port W0/W1 Failed	700 KΩ	700 KΩ

TABLE 2-III
Fault Behaviors of Open Defects for Cell-Sizing-2 of Sub-Category1&2

Property	Transistor Name	Transistor Terminal	Faulty Behavior	Min. Detectable Resistance Of Sub-Category1	Min. Detectable Resistance Of Sub-Category2
A-port pass transistor	M5	G	(SP) A-Port W0 Failed	4 MΩ	4 MΩ
		S/D	(SP) A-Port W1 Failed	70 KΩ	110 KΩ
	M6	G	(SP) A-Port W1 Failed	4 MΩ	4 MΩ
		S/D	(SP) A-Port W0 Failed	70 KΩ	110 KΩ
B-port pass transistor	M7	G	(SP) B-port W0 Failed	4 MΩ	4 MΩ
		S/D	(SP) B-port W1 Failed	70 KΩ	110 KΩ
	M8	G	(SP) B-port W1 Failed	4 MΩ	4 MΩ
		S/D	(SP) B-port W0 Failed	70 KΩ	110 KΩ
Pull-Up transistor	M1	G	(SP) A-Port W0 Failed	3 MΩ	5 MΩ
		S/D	(SP) A-/B-port W1 Failed	30 MΩ	30 MΩ
	M2	G	(SP) A-Port W1 Failed	3 MΩ	5 MΩ
		S/D	(SP) A-/B-port W0 Failed	30 MΩ	30 MΩ
Pull-Down transistor	M3	G	(SP) A-/B-port W1 Failed	3 MΩ	4 MΩ
		S/D	(DP) A-port W0 Failed	300 KΩ	300 KΩ
	M4	G	(SP) A-/B-port W0 Failed	3 MΩ	4 MΩ
		S/D	(DP) A-port W0 Failed	300 KΩ	300 KΩ
Connection	RQ	-	(SP) A-/B-port W0/W1 Failed	1 MΩ	700 KΩ
Connection	RQB	-	(SP) A-/B-port W0/W1 Failed	1 MΩ	700 KΩ

TABLE 2-IV
Fault Behaviors of Open Defects for Cell-Sizing-3 of Sub-Category1&2

Property	Transistor Name	Transistor Terminal	Faulty Behavior	Min. Detectable Resistance Of Sub-Category1	Min. Detectable Resistance Of Sub-Category2
A-port pass transistor	M5	G	(SP) A-Port W0 Failed	3 M Ω	4 M Ω
		S/D	(SP) A-Port W1 Failed	50 K Ω	70 K Ω
	M6	G	(SP) A-Port W1 Failed	3 M Ω	4 M Ω
		S/D	(SP) A-Port W0 Failed	50 K Ω	70 K Ω
B-port pass transistor	M7	G	(SP) B-port W0 Failed	3 M Ω	4 M Ω
		S/D	(SP) B-port W1 Failed	50 K Ω	70 K Ω
	M8	G	(SP) B-port W1 Failed	3 M Ω	4 M Ω
		S/D	(SP) B-port W0 Failed	50 K Ω	70 K Ω
Pull-Up transistor	M1	G	(SP) A-Port W0 Failed	2 M Ω	3 M Ω
		S/D	(SP) A-/B-port W1 Failed	20 M Ω	20 M Ω
	M2	G	(SP) A-Port W1 Failed	2 M Ω	3 M Ω
		S/D	(SP) A-/B-port W0 Failed	20 M Ω	20 M Ω
Pull-Down transistor	M3	G	(SP) A-/B-port W1 Failed	2 M Ω	4 M Ω
		S/D	(DP) A-port W0 Failed	300 K Ω	300 K Ω
	M4	G	(SP) A-/B-port W0Failed	2 M Ω	4 M Ω
		S/D	(DP) A-port W0 Failed	300 K Ω	300 K Ω
Connection	RQ	-	(SP) A-/B-port W0/W1 Failed	700 K Ω	700 K Ω
Connection	RQB	-	(SP) A-/B-port W0/W1 Failed	700 K Ω	700 K Ω

For the sub-category3, we select cell-sizing-3 as the base macro circuit and run Monte-Carlo simulations. There are eight groups of V_{TH} variation and each of them implements the dual-port A-port write-logic-1 and the B-port read-logic-0 operation simultaneously so that DP-SRAM cell suffers the write-disturb issue. Table 2-IV shows the minimum detectable resistance of each open defect (from Column 5 to Column 12) and the preferred test operations (Column 4) for configuration-3 of the sub-category3. The preferred test operations in this table simply note single- or dual- port write operation without detail. It is because each open defect of each V_{TH} variation has its preferred test operations; therefore, it's too complicated to include them all.

Table 2-IV shows that the trend for DP-SRAM cells with V_{TH} variations and the write-assist circuitry (Sub-category3) is a little different comparing to

previous results. In this experiment, it appears that only the open defect on the source/drain terminal of the left pull-up PMOS (M2) are hard to detect and others are relatively easy to detect by the conventional march test. We infer that it is due to the asymmetric V_{TH} characteristic of the transistor in DP-SRAM cell. The asymmetric behavior in this experiment makes the DP-SRAM cell tends to have the dual-port A-port write-logic-1 disturbance easily. In this way M1 PMOS becomes much weaker comparing to M2 PMOS; as a result, the open defect on the source/drain terminal of M1 becomes easier to detect.

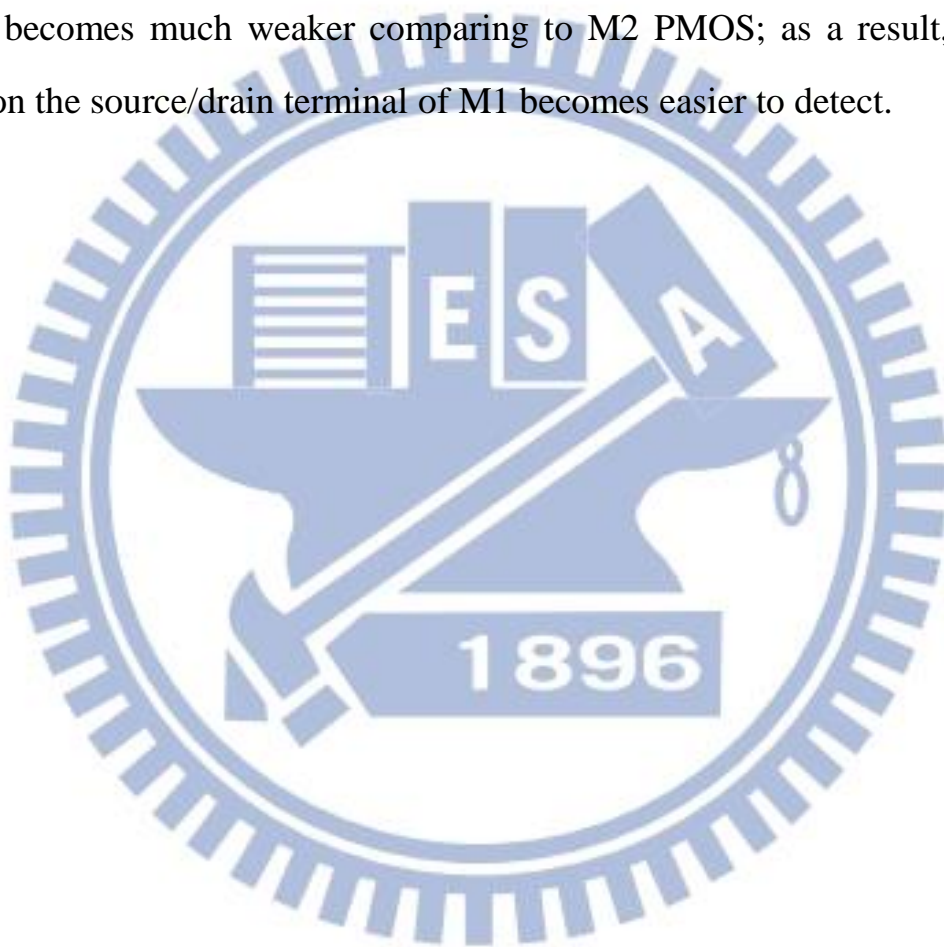


TABLE 2-V
Fault Behaviors of Open Defects for Cell-Sizing-3 of Sub-Category3

Property	Transistor Name	Transistor Terminal	Preferred Test Operations	Min.	Min.	Min.	Min.	Min.	Min.	Min.	Min.	Min.
				Detectable Resistance	Detectable Resistance	Detectable Resistance	Detectable Resistance	Detectable Resistance	Detectable Resistance	Detectable Resistance	Detectable Resistance	Detectable Resistance
A-port pass transistor	M5	G	(SP) W-Failed	6 M Ω	2 M Ω	4 M Ω	9 M Ω	5 M Ω	7 M Ω	3 M Ω	5 M Ω	5 M Ω
		S/D	(SP) W-Failed	10 K Ω	10 K Ω	40 K Ω	50 K Ω	10 K Ω	10 K Ω	10 K Ω	10 K Ω	50 K Ω
		G	(DP) W-Failed	300 K Ω	10 K Ω	500 K Ω	500 K Ω	20 K Ω	300 K Ω	400 K Ω	400 K Ω	200 K Ω
	M6	S/D	(DP) W-Failed	20 K Ω	10 K Ω	30 K Ω	50 K Ω	10 K Ω	20 K Ω	20 K Ω	10 K Ω	10 K Ω
		G	(SP) W-Failed	5 M Ω	2 M Ω	10 M Ω	8 M Ω	4 M Ω	8 M Ω	20 M Ω	20 M Ω	5 M Ω
		S/D	(DP) W-Failed	20 K Ω	10 K Ω	30 K Ω	50 K Ω	10 K Ω	20 K Ω	20 K Ω	10 K Ω	10 K Ω
B-port pass transistor	M7	G	(SP) W-Failed	500 K Ω	3 M Ω	9 M Ω	5 M Ω	2 M Ω	4 M Ω	4 M Ω	6 M Ω	5 M Ω
		S/D	(DP) W-Failed	20 K Ω	10 K Ω	30 K Ω	50 K Ω	10 K Ω	20 K Ω	10 K Ω	10 K Ω	10 K Ω
		G	(SP) W-Failed	500 K Ω	3 M Ω	9 M Ω	5 M Ω	2 M Ω	4 M Ω	4 M Ω	6 M Ω	5 M Ω
	M8	S/D	(SP) W-Failed	40 K Ω	30 K Ω	400 K Ω	300 K Ω	80 K Ω	200 K Ω	300 K Ω	300 K Ω	90 K Ω
		G	(DP) W-Failed	500 K Ω	10 K Ω	700 K Ω	600 K Ω	300 K Ω	600 K Ω	700 K Ω	700 K Ω	300 K Ω
		S/D	(DP) W-Failed	200 K Ω	10 K Ω	300 K Ω	200 K Ω	100 K Ω	400 K Ω	300 K Ω	300 K Ω	60 K Ω
Pull-Up transistor	M1	G	(DP) W-Failed	200 K Ω	10 K Ω	500 K Ω	400 K Ω	70 K Ω	200 K Ω	300 K Ω	300 K Ω	200 K Ω
		S/D	(DP) W-Failed	500 K Ω	10 K Ω	700 K Ω	600 K Ω	300 K Ω	600 K Ω	700 K Ω	700 K Ω	300 K Ω
		G	(SP) W-Failed	30 M Ω	20 M Ω	60 M Ω	50 M Ω	30 M Ω	30 M Ω	40 M Ω	40 M Ω	80 M Ω
	M2	S/D	(DP) W-Failed	200 K Ω	10 K Ω	500 K Ω	400 K Ω	100 K Ω	400 K Ω	300 K Ω	300 K Ω	60 K Ω
		G	(DP) W-Failed	80 K Ω	10 K Ω	300 K Ω	200 K Ω	50 K Ω	60 K Ω	300 K Ω	300 K Ω	200 K Ω
		S/D	(DP) W-Failed	200 K Ω	200 K Ω	500 K Ω	200 K Ω	200 K Ω	300 K Ω	300 K Ω	300 K Ω	200 K Ω
Pull-Down transistor	M3	G	(DP) W-Failed	800 K Ω	30 K Ω	1 M Ω	900 K Ω	400 K Ω	400 K Ω	900 K Ω	400 K Ω	400 K Ω
		S/D	(DP) W-Failed	200 K Ω	200 K Ω	500 K Ω	200 K Ω	200 K Ω	300 K Ω	300 K Ω	300 K Ω	200 K Ω
		G	(DP) W-Failed	400 K Ω	10 K Ω	400 K Ω	500 K Ω	300 K Ω	200 K Ω	500 K Ω	200 K Ω	200 K Ω
	M4	S/D	(DP) W-Failed	50 K Ω	10 K Ω	200 K Ω	200 K Ω	30 K Ω	40 K Ω	90 K Ω	40 K Ω	40 K Ω
		G	(DP) W-Failed	50 K Ω	10 K Ω	200 K Ω	200 K Ω	30 K Ω	50 K Ω	90 K Ω	90 K Ω	40 K Ω
		-	(DP) W-Failed	50 K Ω	10 K Ω	200 K Ω	100 K Ω	30 K Ω	50 K Ω	90 K Ω	40 K Ω	40 K Ω
Connection	RQ	-	(DP) W-Failed	50 K Ω	10 K Ω	200 K Ω	100 K Ω	30 K Ω	50 K Ω	90 K Ω	40 K Ω	
	RQB	-	(DP) W-Failed	50 K Ω	10 K Ω	200 K Ω	100 K Ω	30 K Ω	50 K Ω	90 K Ω	40 K Ω	

2.3.4 Fault Behaviors for Write-Assist Circuitry

In the following experiment, we focus on the open defects for the write-assist circuitry. The structure of the WA8T cell in Figure 2-8 is symmetric. The left part works for the dual-port A-port write-logic-1 operation and the right part works for the dual-port A-port write-logic-0 operation. As a result, the following discussion only focuses on the left part of the WA8T cell which helps suppressing the dual-port write-logic-1 disturbance.

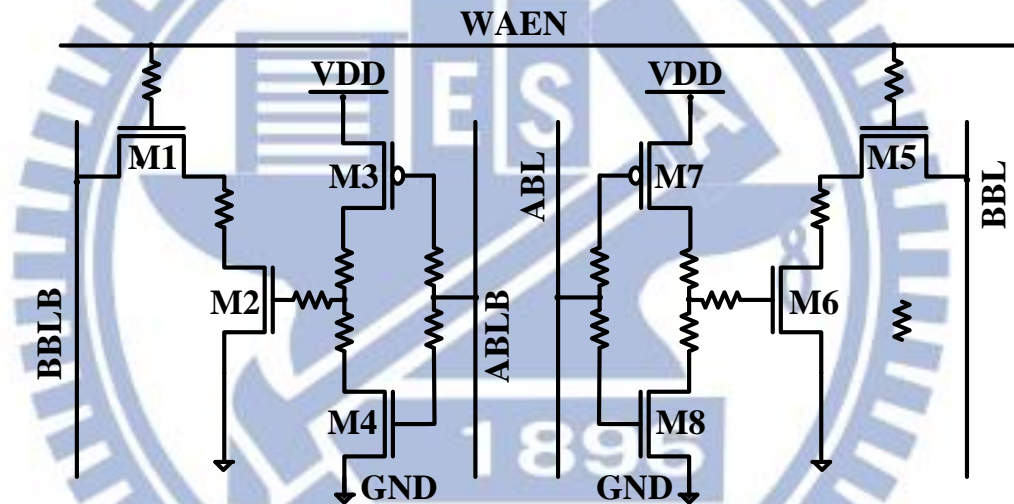


Fig. 2-8 Schematic of the Write-Assist Circuitry (WA8T)

Figure 2-8 shows the defects injection. We inject the open defect with different resistance value one at a time on each terminal (gate or source/drain) of each transistor (M1 to M4). Specially, M1 and M2 share the same resistance as their source/drain open defect. We report the minimum resistance for each open defect under seven V_{TH} variations in table 2-V. These open defects can cause the WA8T cell breaks down and hinder the suppression of the write-disturb issue of DP-SRAM cell.

As table 2-V shows, four open defects highlighted in the gray background are classified as hard to detect faults. Among these four open defects, three of them are on the gate terminal and they are inherently high impedance. The other one is on the source/drain terminal of M4. As a result, we focus on developing test methods for the one on the source/drain terminal first and developing other methods to detect those hard to detect faults last.

TABLE 2-VI
Fault Behaviors of Open Defects for the Write-Assist Circuitry (WA8T)

Transistor Name	Transistor Terminal	Faulty Behavior	Min.	Min.	Min.	Min.	Min.	Min.	Min.
			Detectable Resistance Of Var.1	Detectable Resistance Of Var.2	Detectable Resistance Of Var.3	Detectable Resistance Of Var.4	Detectable Resistance Of Var.5	Detectable Resistance Of Var.6	Detectable Resistance Of Var.7
M1	G	Dual-Port A-port W1 Failed	3 M Ω	300 G Ω	20 M Ω	200 G Ω	200 G Ω	60 G Ω	5 M Ω
	S/D		40 K Ω	2 M Ω	200 K Ω	70 K Ω	100 K Ω	6 M Ω	40 K Ω
M2	G		300 K Ω	6 M Ω	5 M Ω	1 M Ω	1 M Ω	4 M Ω	2 M Ω
	S/D		40 K Ω	2 M Ω	200 K Ω	70 K Ω	100 K Ω	6 M Ω	40 K Ω
M3	G		Undetected	70 K Ω	Undetected	2 M Ω	4 M Ω	3 M Ω	Undetected
	S/D		100 K Ω	2 M Ω	2 M Ω	800 K Ω	800 K Ω	1 M Ω	500 K Ω
M4	G		Undetected	20 M Ω	Undetected	Undetected	Undetected	Undetected	7 M Ω
	S/D		Undetected	Undetected	Undetected	Undetected	Undetected	Undetected	Undetected

Chapter 3

Testing of Write-Assist Dual-Port SRAM and the Proposed Methods

A significant amount of research effort has been put into the area of developing an effective and economic DP-SRAM designs. Consequently, testing of DP-SRAMs has also become more important. In 2002, [2-10] has discussed realistic fault models for DP-SRAMs and it divided them into single-port faults and faults unique for dual-port operations. It concerns about faults that related to the multi-port and simultaneous access behavior for different cells. It states that testing multi-port memories require special tests since the multi-port and simultaneous access can sensitize faults that are different from conventional single-port memory faults.

However, such models become insufficient in deep sub-micrometer technology. We are more interested in the open defects that originate from manufacturing process. The existing testing methodologies are not effective enough for the advanced DP-SRAM design and the new write-assist circuitry and they have not been fully discussed in the literature yet. In this chapter, we will propose several test methods and each method is primarily used for one specific hard-to-detect fault in the chapter2. We develop these methods based on other's works and the dual-port characteristic of DP-SRAMs. In this way, we can reduce the complexity of its DFT. We then compare experiment results to

prove that our methods are in good use. In the end of this chapter, we show the Design-for-Test (DFT) for each different test method.

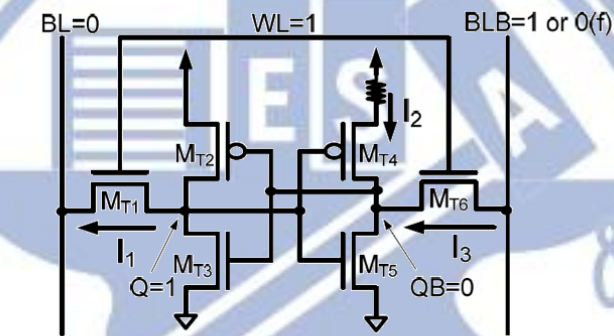
3.1 Testing of the Open Defects in Dual-Port SRAM Core Cell

In this section, we first discuss the severe write method proposed in [2-11]. In our experiments, we found that this method is not useful when testing DP-SRAMs. We propose Half-VDD Attacking Method based on the severe write method to detect the stability faults. It turns out our method is useful for both DP-SRAMs with V_{TH} variations and without V_{TH} variations.

3.1.1 Previous Method – Sever Write Method

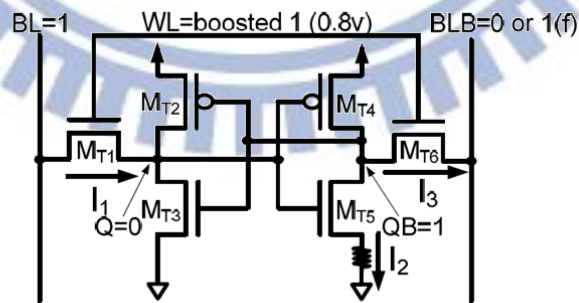
The idea of severe write method [2-11] in 6T SRAM design is performing a write operation by a weaker bit-line supply. Taking write-logic-0 as an example shown in figure 3-1(a), we set BL to strong logic-0 and BLB to floating logic-0 at the test mode (write logic-0 operation) instead of strong logic-0 and strong logic-1 at the normal mode. With such a write operation, writing successfully becomes more difficult since the floating logic-0 is opposite to the target value at Q or QB. If an open defect falls on the source/drain terminal of PMOS transistors (M_{T2} and M_{T4}), it weakens the pull-up ability of the cross-couple inverters. Accordingly, the cell will fail to write the correct data and the open defect can be detected. Figure 3-1(a) illustrates how the severe write method can help the detection of an open defect on the pull-up PMOS.

In fact, the severe write method for the pull-up PMOS can also be modified to detect open defects on the source/drain terminal of NMOS transistors by setting BL to strong logic-1 and BLB to floating logic-1, as shown in figure 3-1(b). Such a severe write condition can activate the open defect successfully. However, it needs to boost the voltage at the WL by one V_{TH} to enhance the ability of passing a logic-1 value through the NMOS pass transistor during the test mode. Figure 3-1(b) illustrates how this refined version of the severe write method can help the detection of an open defect on the NMOS transistor M_{T5} .



W0 with initially Q=1 & QB=0					
Normal write			Severe write		
BL=0	Q =1 →0	$I_1 > 0$	BL=0	Q=1 →0	$I_1 > 0$
BLB=1	QB=0 →1	$I_2 > 0$ $I_3 > 0$	BLB=0(f)	QB=0 →1	$I_2 > 0$ $I_3 \leq 0$

(a) Severe write for testing pMOS stability fault



W1 with initially Q=0 & QB=1					
Normal write			Severe write		
BL=1	Q =0 →1	$I_1 > 0$	BL=1	Q=0 →1	$I_1 > 0$
BLB=0	QB=1 →0	$I_2 > 0$ $I_3 > 0$	BLB=1(f)	QB=1 →0	$I_2 > 0$ $I_3 \leq 0$

(b) Severe write for testing nMOS stability fault

Fig. 3-1 Illustration of Severe Write Method [2-11]

3.1.2 Proposed Method – Half-VDD Attacking Method

This method is mainly used for the open defect on the source/drain terminal of the pull-up PMOS in the cross-couple inverter in figure 3-2. The idea of this method is based on the severe write method [2-11]. In our experiment, severe write method makes the defect-free DP-SRAM cell can't write successfully and therefore we can't detect a reasonable minimum resistance for each open defect. We infer that it is because the sizing rule of our cell design makes pull-down NMOS transistors too strong so that the storage node originally stored at logic-0 level will be clamped strongly. In the end, the severe write operation fails for the defect-free DP-SRAMs. We also perform the experiment that by setting the BL to strong logic-0 level and the BLB floating logic-1 level at the test mode (We called it "floating write method" here). The result for the minimum detectable resistance shows that it makes no improvement comparing to normal write operation. For this reason, we believe that we can find an appropriate solution in between.

Figure 3-2 illustrates half-VDD attacking method. We modified the write logic-0 operation by setting ABL to strong logic-0 and ABLB floating 0.5VDD at the test mode, instead of strong logic-0 and floating logic-0 in the severe write method. Through our experiment, it shows that it is useful to detect the open defect on the source/drain terminal of the pull-up PMOS for both with- V_{TH} -variations and without- V_{TH} -variations conditions. There are two modes of the proposed method. One is operating in the single-port mode, figure 3-2(a) and the other is operating in the dual-port mode, figure 3-2(b). The former one is used for DP-SRAM cells without V_{TH} variations and the later one is used for DP-SRAM cells with V_{TH} variations.

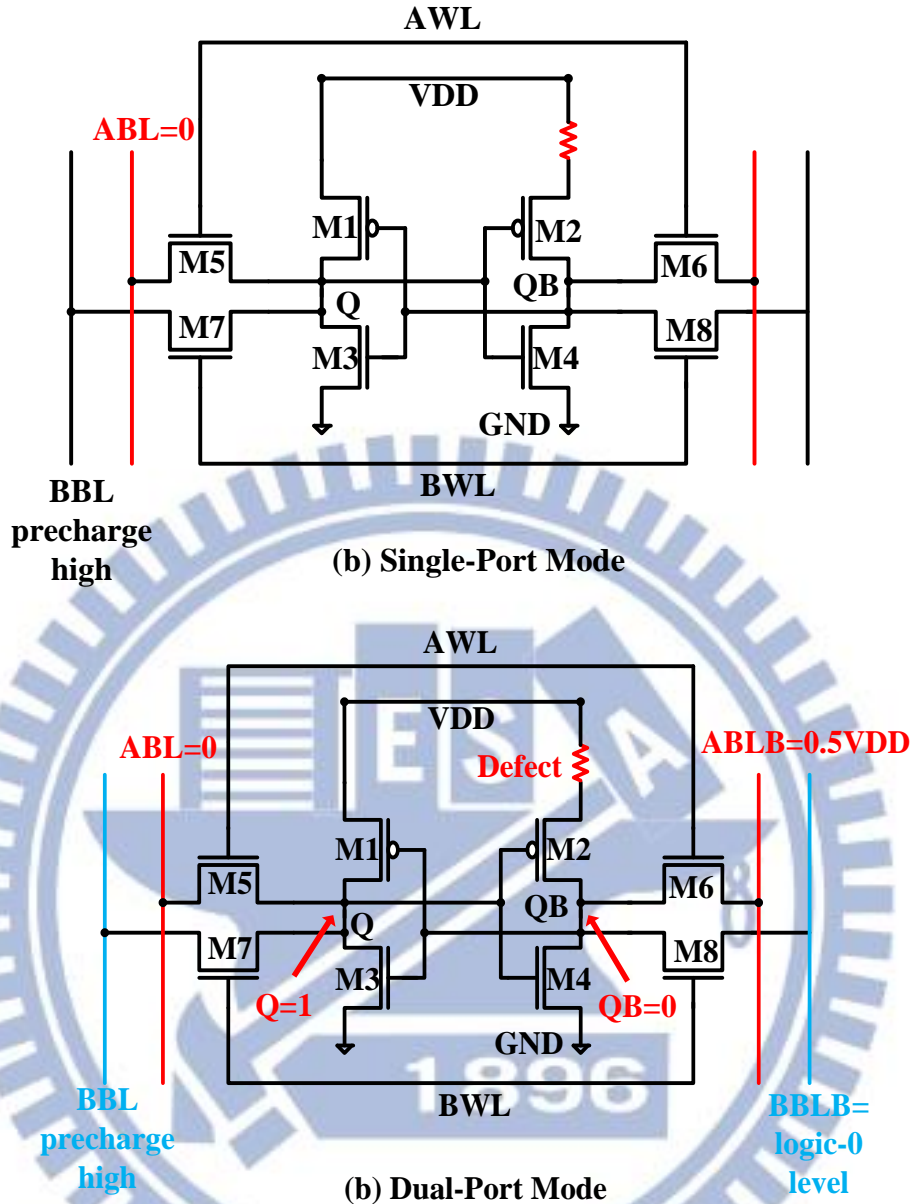


Fig. 3-2 Illustration of Half-VDD attacking Method

3.1.3 Experiment Results and Comparison

Table 3-I shows the effectiveness of different test methods for the source/drain open defect of sub-category1 and sub-category2 together. (Sub-category1 represents DP-SRAM cell without V_{TH} variation and without WA8T cell and sub-category2 represents DP-SRAM cell with V_{TH} variation and

without WA8T cell). The minimum detectable resistance for both sub-category1 and sub-category2 is the same because the single-port mode would not activate the WA8T cell. Three different cell-sizing are experimented in order to prove the effectiveness of the proposed half-VDD attacking method. We use the single-port mode for DP-SRAMs without V_{TH} variations instead of the dual-port mode because the latter one would be too aggressive as stated before and it may cause over-test problems. Thus, using the single-port mode for DP-SRAMs without V_{TH} variations would be the optimum solution.

We also consider the voltage drift situation of half-VDD attacking method. The situation may happen because the capacitance of different bit-lines is not perfectly equal and the timing of the control signal may have skews when the process variation happens. Therefore, we perform three cases of the bit-line voltage drift, +10% voltage drift (412.5 mV), no voltage drift (375mV) and -10 % voltage drift (337.5 mV), to show that the proposed method sustains a reasonable range of the voltage drift. The label “-” in table 3-I represents the situation that severe write method would fail the write operation for defect-free DP-SRAM cells. The results show that we can detect the open defect by one-order lesser in average and the detected resistance would maintain an acceptable range when the voltage drift situation occurs.

TABLE 3-I
Effectiveness of Different Test Methods for the S/D Open Defect of
Sub-Category1&2

MI (S/D)	Config.1	Config.2	Config.3
Write + Read	20 MΩ	30 MΩ	20 MΩ
(SP) Floating Write	20 MΩ	30 MΩ	20 MΩ
(SP) Severe Write	-	-	-
(SP) +10% Half-VDD Attacking	3.7 MΩ	4.8 MΩ	2.7 MΩ
(SP) + 0% Half-VDD Attacking	2.4 MΩ	3.0 MΩ	1.8 MΩ
(SP) -10% Half-VDD Attacking	1.4 MΩ	1.8 MΩ	840 KΩ

Table 3-II shows the effectiveness of different test methods for sub-category-3. We use the configuration3 macro in this experiment and the dual-port mode of half-VDD attacking method is applied rather than the single-port mode. It is because DP-SRAMs with V_{TH} variations are asymmetric inherently and the single-port method would not be effective enough to test these open defects. In contrast, the dual-port mode makes write operation more severe so that we can detect the open defects easier. The dual-port mode not only supplies strong logic-0 at ABL and floating 0.5VDD at ABLB at the test mode (write logic-0 operation), but also supplies an additional disturb source from B-port. This method can only be performed for DP-SRAMs owing to its natural dual-port structure.

From table 3-II, we prove that the dual-port method is more efficacious than the single-port mode. The resistance detected by the single-port mode is at the same order or even higher comparing to the W-R operation (row1) and the resistance detected by the dual-port mode appears to be two-order lesser in average. Also, we perform the voltage drift experiment for both modes to insure our method withstand a reasonable range of voltage fluctuation. To sum up, it is convincing to use half-VDD attacking method for the source/drain open defect

of the PMOS in DP-SRAMs. The label “-” in the table 3-II represents the situation that severe write method would fail the write operation for defect-free DP-SRAM cells.

TABLE 3-II
Effectiveness of Different Test Methods for the S/D Open Defect of
Sub-Category 3 for Configuration3

M1 (S/D)	Var.1	Var.2	Var.3	Var.4	Var.5	Var.6	Var.7	Var.8
Write + Read	30 MΩ	20 MΩ	60 MΩ	40 MΩ	30 MΩ	20 MΩ	40 MΩ	70 MΩ
(SP) Floating Write	20 MΩ	30 MΩ	20 MΩ	20 MΩ	30 MΩ	20 MΩ	20 MΩ	20 MΩ
(SP) Severe Write	-	-	-	-	-	-	-	-
(SP) +10% Half-VDD Attacking	100 MΩ	20 MΩ	20 MΩ	300 MΩ	40 MΩ	50 MΩ	40 MΩ	20 MΩ
(SP) + 0% Half-VDD Attacking	40 MΩ	8 MΩ	10 MΩ	40 MΩ	20 MΩ	30 MΩ	20 MΩ	10 MΩ
(SP) -10% Half-VDD Attacking	20 MΩ	6 MΩ	6 MΩ	20 MΩ	10 MΩ	20 MΩ	20 MΩ	6 MΩ
(DP) +10% Half-VDD Attacking	900 KΩ	200 KΩ	300 KΩ	700 KΩ	600 KΩ	800 KΩ	800 KΩ	80 KΩ
(DP) + 0% Half-VDD Attacking	800 KΩ	90 KΩ	100 KΩ	600 KΩ	500 KΩ	700 KΩ	700 KΩ	50 KΩ
(DP) -10% Half-VDD Attacking	700 KΩ	60 KΩ	60 KΩ	500 KΩ	400 KΩ	700 KΩ	500 KΩ	50 KΩ

3.2 Testing of the Open Defects in Write-Assist Circuitry

The proposed methods are used for the open defects of the write-assist circuitry. Two test methodologies are proposed and they are used independently for different targets. The first one is low-voltage write-assist method and the second one is severe read method. The following sections will discuss these methods and their experiment results.

3.2.1 Proposed Method – Low Voltage Write-Assist Method

This method is used to detect the open defect on the gate terminal of M1 and M5 NMOS of the WA8T cell. The method is based on the following idea. The write-assist circuitry enable signal (WAEN) controls the whole WA8T to work or not and it is directly connected to the M1/M5 NMOS as shown in figure

3-3. Hence lowering the voltage of the WAEN signal may bring about the reduction of turn-on current of M1/M5 NMOS and weakens the ability of the write-assist circuitry. In this way, the open defect on the gate terminal of M1/M5 NMOS can be detected more easily.

3.2.2 Proposed Method – Severe Read Method

The method is used to detect the open defect on the source/drain terminal of M4 NMOS as shown in figure 3-3. This idea is based on the dual-port characteristic of DP-SRAMs. We try to read the cell value from one port and disturb it from the other port. The disturbance is created with the help of the WA8T cell. In this way, we can observe the open defect more effectively.

The method is performed in the following way. In the first stage, it performs the single-A-port write-logic-0 operation to initiate the cell value at logic-0. In the second stage, it performs the single-A-port write-logic-1 operation with word-line-A (WLA) turn off. This modified write operation charges the node N1 to a floating-logic-1 level and it is not a real write operation. In the third stage, a modified single-B-port read-logic-0 operation is performed. It reads the cell value on to B-port word-lines first and inserts an A-port disturb operation before B-port sense amplifier is activated. The A-port disturb operation performs a modified single-port write-logic-1 operations with the word-line-A (WLA) being turned off and the WAEN signal being turned on specially. The modified write-logic-1 operations set ABL and ABLB both to logic-1. This operation would discharge the node N1 to logic-0 level and disconnect the discharge path formed by M1 and M2 NMOS. However, if the open defect happens, the node N1 will not be pulled down to logic-0 level at the end of the third stage due to

the wrong discharge path for BBLB. Lastly the B-port sense amplifier is on and sense out data from B-port bit-line pairs. We would read a correct data if no defects happen and a wrong data in the opposite. Figure 3-3 is an illustration of severe read method.

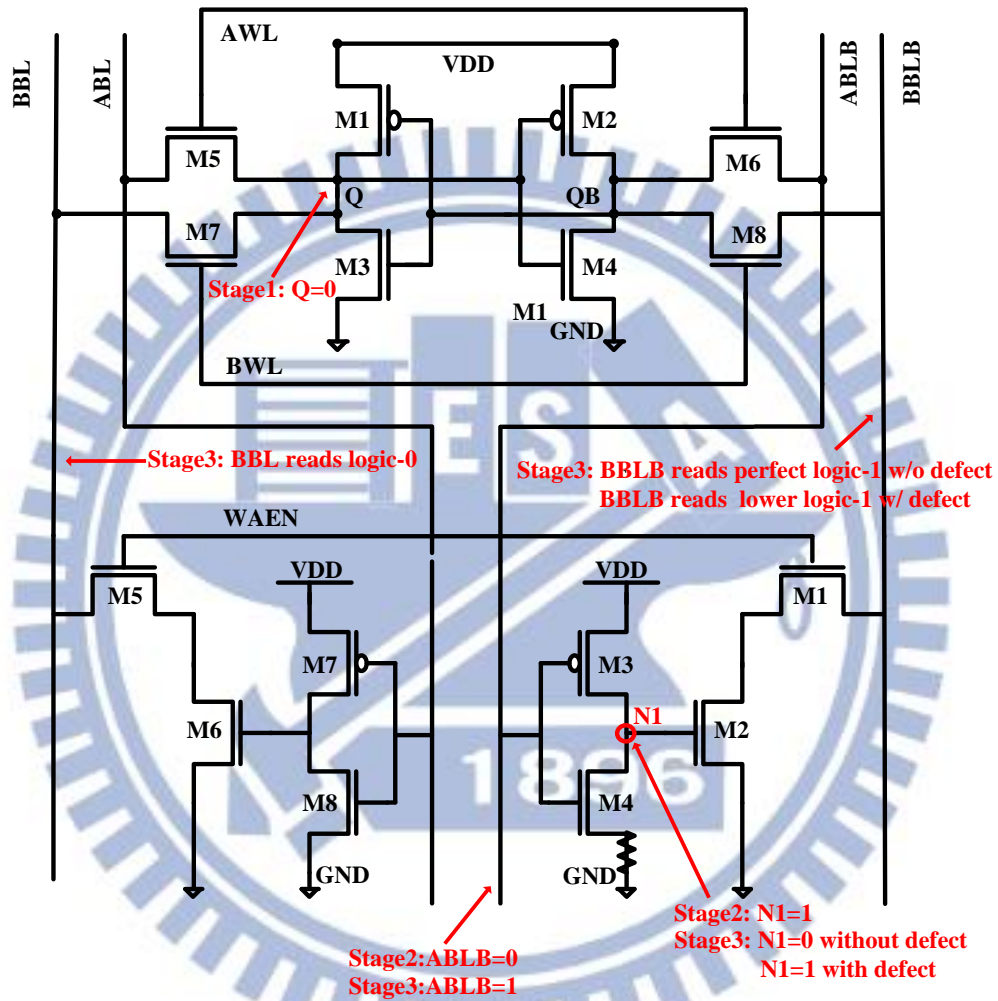


Fig. 3-3 Illustration of Severe Read Method

3.2.3 Experiment Results and Comparison

Table 3-III shows the experiment result of low-voltage write-assist method. The label ‘-’ represents the situation that the method would fail write operations for defect-free WA8T cell. We sweep different WAEN voltage level for every V_{TH} variation. We find that 90% of the WAEN voltage level is enough for most

cases. Using too aggressive voltage level may result in the write failure for those defects originally detected in smaller resistance. The results show that we can detect lower resistance of the open defect by at least one-order lesser for normal cases or even more greater for some extreme case.

TABLE 3-III
Experiment Result for the Gate Terminal Open Defect of the WA8T

Gate terminal of M1	Var.1	Var.2	Var.3	Var.4	Var.5	Var.6	Var.7
Write + Read	3 M Ω	300 G Ω	20 M Ω	200 G Ω	200 G Ω	60 G Ω	5 M Ω
Low-Voltage WAEN at 90%	-	8 M Ω	7 M Ω	5 M Ω	5 M Ω	8 M Ω	4 M Ω
Low-Voltage WAEN at 80%	-	8 M Ω	7 M Ω	3 M Ω	4 M Ω	8 M Ω	-
Low-Voltage WAEN at 70%	-	8 M Ω	5 M Ω	-	-	8 M Ω	-
Low-Voltage WAEN at 60%	-	5 M Ω	-	-	-	5 M Ω	-

Table 3-IV shows the experiment result of the Severe Read Method. We sweep every V_{TH} variation to prove the effectiveness of the method. These open defects are originally undetected in all cases and we are able to detect them from fifty-mega ohm to sixty-mega ohm in each case.

M4-MOS is used to guarantee the voltage level of the node N1 in figure 3-3 is at logic-0 level during the pre-charge operation and the dual-port write-logic-1 operation. The node N1 controls the discharge path of BBLB for the dual-port write-logic-1 operation. If the open defect happens, some operating sequence would activate the WA8T cell at the wrong time making the WA8T a burden instead of assistance. However, the WAEN signal is turned off in the pre-charge operation making the open defect on the source/drain terminal of M4 unable to detect. Therefore, we try to detect the open defect by the dual-port write-logic-1 operation combining with the read operation. This would be an efficient way to detect the open defect.

Table 3-IV
Experiment Result for the S/D Terminal Open Defect of the WA8T

S/D terminal of M4	Var.1	Var.2	Var.3	Var.4	Var.5	Var.6	Var.7
Write + Read	U.D.	U.D.	U.D.	U.D.	U.D.	U.D.	U.D.
Severe Read Method	50M	60M	60M	50M	60M	60M	60M

3.3 Design-for-Test for the Proposed Methods

In this section we discuss the Design-for-Test of each proposed method. We first begin with the DFT for half-VDD attacking method and then we show the DFT for low-voltage write-assist method. Through our discussion, the proposed method is applicable in reality. We also discuss the area overhead problem for both of them. The area overhead both turns out to be less than 1%. For severe read method, we simply modify the operating sequence; therefore, we do not discuss the Design-For-Test, because its DFT is incorporated into the timing control unit and the area overhead is very small. Therefore, it is not discussed in the following page.

3.3.1 DFT for Half-VDD Attacking Method

In order to produce a half-VDD voltage, we make use of the dual-port structure of DP-SRAMs. We pre-charge one pair of the bit-lines to the VDD level as normal operation did and pre-charge the other pair to the ground level in the pre-charge period. We add one equalizer as the DFT between the two independent bit-line pairs. The equalizer would be turned on by the EN_Equal signal in the beginning of the write operation for a small period of time. This

period determines how accurate of half-VDD voltage would be; therefore, we need to control the period carefully. Figure 3-4 is an illustration of the DFT by the half part of DP-SRAM cell.

For each column, we need two NMOSs as the DFT. Accordingly, the area overhead for each column would be about 0.2% which is pretty small. The power issue is also being considered. The DFT has no direct DC current path; therefore it would not produce amount of power issue. Regarding the pre-charge to ground operation, we can achieve it with additional pre-charge circuits. The circuits is simple and is not discussed here.

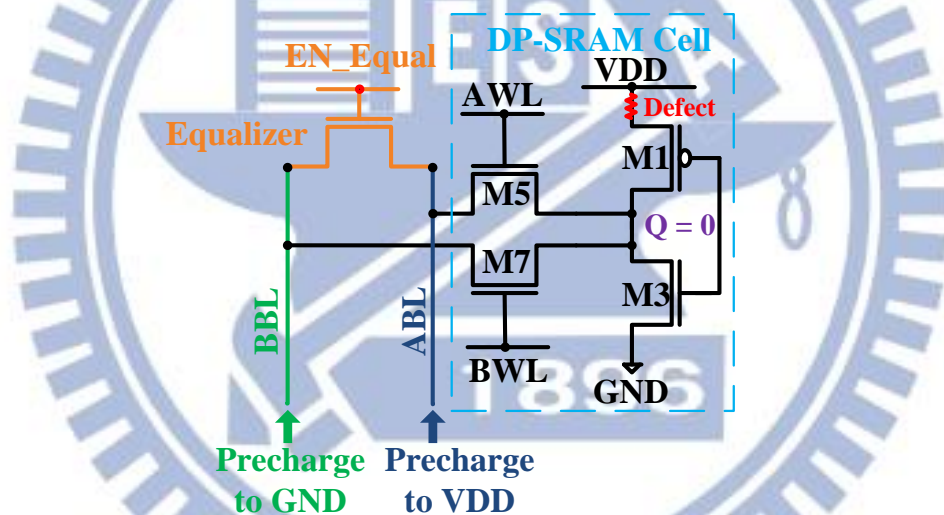


Fig. 3-4 Illustration of the DFT for Half-VDD Attacking

Table 3-V

Half-VDD Attacking Operating Flow

Stage1	Precharge ABL and ABLB to VDD. Precharge BBL to GND and BBLB to VDD.
Stage2	Turn on Equalizer (EN_Equal=1) before A-port write logic-1 operation.
Stage3	Perform write operation: ABL = floating-0.5VDD, ABLB = strong logic-0 BBL = around floating logic-0 level, BBLB = floating logic-1

Table 3-VI
Comparison of Voltage State for Half-VDD Attacking

Write logic-1 operation	Before Equalization	After Equalization
ABL	Floating-1	0.5VDD level
BBL	Floating-0	Around logic-0 level

3.3.2 DFT for Low-V Write-Assist Enable Method

In order to lower the write-assist enable signal to 90% VDD voltage level, we add an extra transmission gate between the External_WAEN signal and the gate terminal of M1-NMOS, WAEN. Figure 3-5 illustrates half of the WA8T cell and the corresponding DFT. The control signal of the transmission gate is both connected the TX_EN signal. The TX_EN signal would be at logic-1 level only for the test mode and logic-0 level for the normal mode. Specially, the voltage of the TX_EN is connected to the V_{SUPPLY} , which is the overall external supply voltage (1.05V) instead of the VDD as before (0.75V). When in the test mode, only the NMOS in the transmission gate is turned on. As NMOS is not suitable for passing a logic-1 value, the voltage level of the gate terminal of M1 would be reduced by one threshold voltage (about 400mV) so that we can achieve our ideal suppressed voltage level. On the contrary, the voltage level of the gate terminal of M1 would be perfect logic-1 in the normal node because the PMOS in the transmission gate is suitable for passing logic-1 value. We can attain our target voltage level by this way.

As shown in figure 3-5, we need one transmission gate for all a-port and one transmission gate for all b-port. It means we need four transistors for overall

memory bank. Because the memory bank is 128X128 cells, the area overhead for the DFT is about 3.05×10^{-5} which is less than 1%.

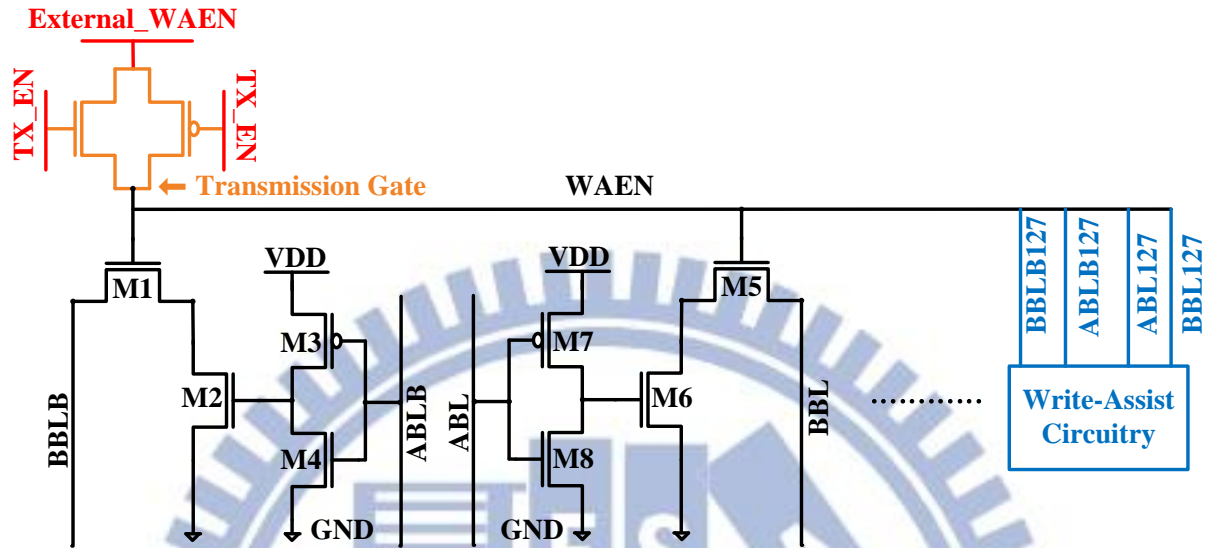


Fig. 3-5 Illustration of the DFT for Low-V WAEN

**Table 3-VII
Operations of Low-V Write-Assist**

Operation	Behavior	Voltage of WAEN
TX_EN = 1	NMOS turn on and pass a weak logic-1 to WAEN	About 650mV
TX_EN = 0	NMOS turn on and pass a strong logic-1 to WAEN	1.05V

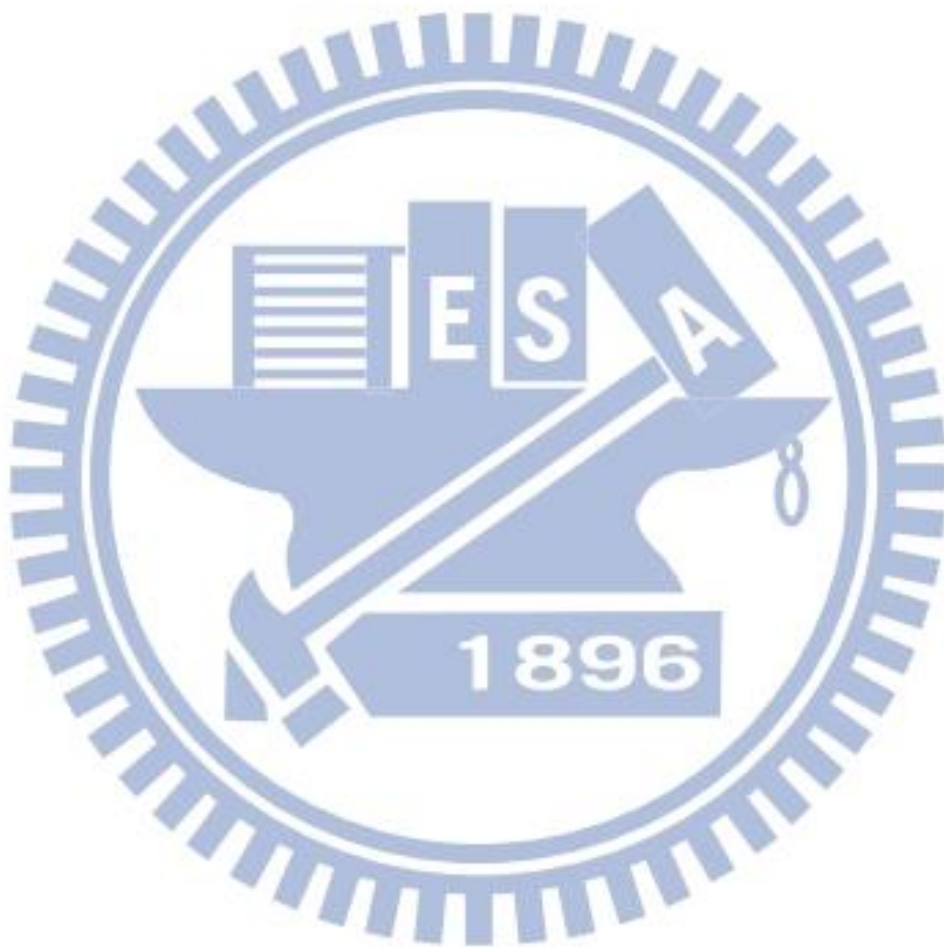
Chapter 4

Conclusion

In this thesis, testing of Dual-Port SRAMs with the write-assist circuit is discussed. We set the experiment on 28nm technology node and simulate the disturb issues as well. We use the newest write-assist circuit as the solution to fix the disturb issue. The open defects in DP-SRAM may cause DP-SRAMs fail to operate correctly and open defects in the write-assist circuitry let DP-SRAMs fail to perform the simultaneous access operation correctly because write-assist circuit fails to suppress the write-disturb issue. Hence, it is important to develop useful methodologies to detect them for further diagnosis and information feedback. Besides, two different targets can be concluded. For DP-SRAM cells, once we detect the open defects beforehand, we can decide whether we should use dummy row or column to repair them or not depending on the cost issue and so on. For the write-assist circuitry, it is even more important. We decide whether we should fix these defects afterward or not. If the write-disturb issue is very severe in one product, it is essential to equip with the write-assist circuitry to suppress the disturbance.

We proposed several test methodologies for the hard-to-detect faults. Half-VDD attacking method is a promising solution for the open defect on the source/drain terminal in DP-SRAM cells. Low-V write-assist method and severe read method are new test method for the write-assist circuitry. Our experiment

results show that we can detect these open defects in a smaller resistance representing better efficiency. DFTs for each proposed method are also discussed in the last and they turn out to be an applicable structure. To sum up, the detectable resistance of open defects can be further lowered by one order to two orders in average comparing to the conventional test algorithm.



Bibliography

- [2-1] J.J. Wu, M.F. Chang, S.W. Lu, and et al., "A 45-nm Dual-Port SRAM Utilizing Write-Assist Cells Against Simultaneous access Disturbance," P. 790-794, IEEE Transactions on Circuits and Systems II: Express Briefs, 2012.
- [2-2] K. Nii, Y. Tsukamoto, M. Yabuuchi, and et al., "Synchronous Ultra-High-Density 2RW Dual-Port 8T-SRAM With Circumvention of Simultaneous Common Row-Access," P. 977-986, IEEE Journal of Solid-State Circuits, 2009.
- [2-3] Y. Ishii, H. Fujiwara, K. Nii, and et al., "A 28-nm dual-port SRAM macro with active bitline equalizing circuitry against write disturb issue," P. 99-100, IEEE Symposium on VLSI Circuits, 2010.
- [2-4] Y. Ishii, H. Fujiwara, T. Doguchi, and et al., "A 28nm dual-port SRAM macro with screening circuitry against write-read disturb failure issues," P. 2535-2544, IEEE Journal of Solid-State Circuits, 2011.
- [2-5] D.P. Wang, H.J. Liao, H. Yamauchi and et al., "A 45nm Dual-Port SRAM with Write and Read Capability Enhancement at Low Voltage," IEEE International SOC Conference, 2007.
- [2-6] L. Dilillo, P. Girard, S. Pravossoudovitch, and et al., "Data Retention Fault in SRAM Memories: Analysis and Detection Procedures," IEEE VLSI Test Symposium, 2005.
- [2-7] J. Yang, B. Wang, Y. Wu, and et al., "Fast Detection of Data Retention Faults and Other SRAM Cell Open Defects," P. 167-180, IEEE Transactions on Computer-Aided Design of Integrated Circuits and Systems, 2006.
- [2-8] A. Pavlov, M. Azimane, J. P. De Gyvez, and et al., "Word Line Pulsing Technique for Stability Fault Detection in SRAM Cells," IEEE International Test Conference, 2005.
- [2-9] A. Ney, L. Dilillo, S. Pravossoudovitch and et al., "A New Design-for-Test Technique for SRAM Core-Cell Stability Faults," Design, Automation & Test in Europe Conference & Exhibition, 2009.
- [2-10] S. Hamdioui and Ad j. Van De Goor, "Efficient Tests for Realistic Faults in Dual-Port SRAMs," P. 460-473, IEEE Transactions on Computers, 2002.
- [2-11] C.W. Lin, H.H. Chen, H.Y. Yang and et al., "Fault Models and Test Methods for Subthreshold SRAMs," P. 1-10, ITC, 2010.